ISES solar world congress | 2011

ISES
International
Solar Energy
Society

www.swc2011.org

Proceedings

August 28 - September 2, 2011
Kassel, Germany

Conference Themes

Solar Heating and Cooling | Solar Buildings | Renewable Electricity | Rural Energy Supply
Resource Assessment | Renewable Energies and Society

Resource Forecasting and Technical Potential

Solar Radiation Availability and Variability

Solar Access Variations in Mixed Urban Fabrics_Levent Case
E. Sakinc

Solar and Coincident Weather Data for Large Scale Solar Deployment in Australasia
T. Lee, W. Logie

Solar Atlas for the Southern and Eastern Mediterranean
C. Hoyer-Klick, H. Allal, A. Bida, P. Blanc, M. Caner, T. Cebecauer, T. Huld, L. Lorych, M. Mahmoud, L. Menard, D. Puig, C. Schillings, M. Schroedter-Homscheidt, M. Suri, L. Wald, T. Wanderer, E. Wey

Solar Energy Potential of an Urban Housing Estate in London
U. Iweala, L. Brotas

Solar Radiation and Uncertainty Information of Meteonorm 7
J. Remund, S. Müller

Solar Radiation Measurement Net at Uruguay
J. Cataldo, P. Galione, P. Pena, P. Toscano

Spatial & Temporal Characteristics of Solar Radiation Variability
R. Perez, T. Hoff, S. Kivalov

Using Sunshine Duration and Satellite Images to Estimate Daily Solar Irradiation on Horizontal Surface
S. Ener Rusen, B.G. Akinoglu, A. Hammer

SOLAR IRRADIATION ASSESSMENT IN URUGUAY USING TARPLEY'S MODEL AND GOES SATELLITE IMAGES

R. Alonso Suárez[a,1], G. Abal[a,2], R. Siri[a], P. Musé[b] and P. Toscano[b]

[a] Instituto de Física and [b] Instituto de Ingeniería Eléctrica,
Facultad de Ingeniería, Universidad de la República
CC 30, Montevideo, Uruguay

1. Introduction

The estimation and characterization of incident solar energy typically involves decades of careful measurements and modeling. In Uruguay, a country with no conventional energy resources (such as coal, oil, natural gas or potentially fissible materials), this process has been initiated only recently. The first systematic efforts on a nation-wide scale resulted in 2009 in the first Solar Map, based on pre-existing long-term daily irradiation data from just three sites, two of which equipped with fotovoltaic sensors Abal et al. (2010). These irradiation measurements were correlated with long-term daily sunshine duration records from the national meteorological service (DNM) network, using the well-established Angström–Prescott methodology Angström (1924); Prescott (1940). This procedure allowed to estimate monthly averages of daily global irradiation, at twelve sites distributed over the country. This information was presented graphically, using standard interpolation techniques as twelve monthly mean irradiation maps with a spatial resolution of about 200 km. The estimated uncertainties were evaluated between 14% and 19 % of the mean, depending on location and month of the year. This initial effort made clear that new controlled quality measurements were urgently required to obtain reliable data on several points of the target territory. A nation-wide program leading to the establishment of several automatic measuring stations equipped with Kipp & Zonen CMP6 field pyranometers was launched from the national University (UdelaR) and is now in operation Toscano and Cataldo (2011). The first years of controlled global irradiance measurements are now available and a preliminary comparison with the estimates of the Solar Map is being reported in D'Angelo et al. (2011).

In a relatively small country such as Uruguay, the spatial resolution with which the solar resource is known is an important concern. The spatial and temporal resolution which can be obtained from methodologies based on correlating global solar irradiation with other sparse ground-data, is very limited. On the other hand, detailed cloud cover information is available from satellite images. This information can be used with a suitable model to generate irradiation estimates over the whole target territory, with a spatial resolution of few kilometers. This work reports an initial step taken in this direction. Starting with a local implementation of Tarpley's statistical model and GOES satellite imagery, global irradiation over the whole target territory is estimated on an hourly, daily and monthly basis for the period 2010-2011. These estimates are compared to new independent ground measurements from three sites which differ from the sites used to adjust the model. We obtain root mean square deviations (rms) of 7% of the mean for monthly averages and less than 12% for daily totals. These results represent a significant improvement over previous irradiation estimates for the target territory and are very encouraging, considering that several refinements to the model are still pending. In spite of its good balance between performance and simplicity, Tarpley's model, as most statistical solar irradiation models, requires local monitoring and eventual recalibration. We consider this work as a step towards the ultimate goal: using satellite imagery with a fine-tuned physical radiation–transfer model to provide a reliable real-time estimation of solar irradiation valid for the southeren part of South America.

This work is organized as follows: Section 2 describes the new solar irradiation measurements used for this work. These data are grouped into two disjoint sets, the training and the evaluation sets. Details on the 10-year database of GOES satellite images, part of which were used for this work, are also provided in this section. Tarpley's model is described in Section 3, including a brief discussion of previous

[1] email: rodrigoa@fing.edu.uy (R. Alonso)
[2] email: abal@fing.edu.uy (G. Abal)

implementations and their reported performance. Our local implementation of Tarpley's model is also described in detail in this section. Finally, our irradiation estimates on an hourly, daily and monthly basis are compared with new ground data in Section 4. A summary of our conclusions is presented in Section 5.

2. Description of the data

Solar irradiation measurements were collected from six ground stations distributed over the whole Uruguayan territory, during the years 2010 and 2011. The data from three of these stations were used to train the model and derive its parameters. The rest of the stations were used to assess the model's performance. In the remainder of this section we provide detailed information on each of these data sets.

2.1 GOES images

We use a local image data bank for the GOES-East geostationary satellite operated by NOAA/NASA at longitude 75° West. The actual physical device operating as GOES-East has changed over time, see Table 1. An image from South America is produced approximately every 30 minutes. More than ten years (2000 to date) of geo-referenced 16–bit NetCDF images (restricted to daylight periods) were downloaded from NOAA's CLASS website (http://www.class.noaa.gov). All bands (one visible and four infrared) were acquired at the highest available resolution. The images in the GOES VIS channel can be thought of as monochromatic photographs of the Earth and clouds as seen from outer space. Since the geographical target for this work is the Uruguayan territory, the geographical window of the images is restricted to latitudes between 29°S to 36°S and longitudes between 53°W and 59°W, as shown in Fig. 1. Within this window, the spatial resolution of the VIS channel is approximately 2 km^2 per pixel. As mentioned before, our database for GOES-East includes images from three different physical radiometers mounted on the GOES 8, GOES 12 and GOES 13 satellites. The number of images from each satellite is shown in Table 1.

Table 1: Composition of the local GOES data bank, part of which was used for this work. There are also a few GOES 13 images in the period 12/2008 to 01/2009. The data bank continues to be updated today, but we have considered images dated prior to 01/07/2011 for this work. For more details, see http://www.class.noaa.gov

Satellite	Start date	End date	images
GOES 8	01/01/2000	01/04/2003	24770
GOES 12	01/04/2003	14/04/2010	50939
GOES 13	14/04/2010	30/06/2011	9586
Total	01/01/2000	31/07/2011	85295

The radiometers in the GOES series have a resolution of 10 bits, so the images are arrays of dimensionless brightness counts which may be scaled to the $[0, 1023]$ range. These images are uncalibrated and they should be corrected using post-launch correction factors and other time-dependent factors which compensate the gradual degradation of the radiometer over time. Since we have not yet calibrated our images, all images used for this work are from the GOES 13 satellite. These images cover the relatively short period since 4/2010 to present day, so we effectively ignore the sensor degradation that may take place over this time period. The use of uncalibrated images from different radiometers (or from the same radiometer, over several years) has been identified as an important source of error in solar irradiation estimates obtained from Tarpley's model.

Figure 1: Left: political map of South America. Right: Zoom showing the target territory for this work and the location of the measurement stations used as training (red) and evaluation (green) sets in our implementation of Tarpley's model. See Tables 2 and 3 for the precise location of the measurement stations.

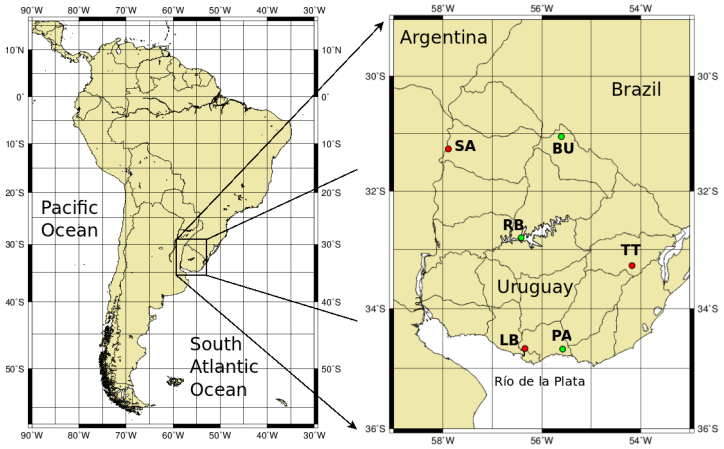

2.2 Ground measurements

The map in Fig. 1 shows the geographical distribution of the measurement stations considered for this work. Only the data collected in the time range where GOES 13 images were available were considered. The three stations that were used to adjust Tarpley's model are equipped with new Kipp and Zonen CM6 pyranometers, and are located at sites of the National Institute for Agronomical Research (INIA) and maintained by our group. The three stations used to evaluate the model are equipped with new Li-Cor LI200SZ fotovoltaic sensors and are owen and operated by UTE, the public electric utility company. More details on the location and time period are presented in Tables 2 and 3. The map in Fig. 1 shows the geographical distribution of the measuring stations considered in this work and the details of the data series are provided in Tables 2 and 3.

Table 2: Details of the measuring stations used for the training data set. Each of them is equipped with a new Kipp & Zonen CMP6 field pyranometer. *Altitude* is expressed as meters over mean sea level. The latitude is in decimal degrees (South) and the longitude in decimal degrees (West).

training site	**code**	**latitude**	**longitude**	**alt.** (m)	**time period**
Las Brujas	LB	-34.672	-56.340	32	02/2010 :: 05/2011
Treinta y Tres	TT	-33.275	-54.172	100	05/2010 :: 05/2011
Salto	SA	-31.273	-57.891	50	06/2010 :: 05/2011

Table 3: Details of the measuring stations used in the evaluation data set. They all use new Li-Cor LI200SZ fotovoltaic sensors. The latitude is in decimal degrees (South) and the longitude in decimal degrees (West).

test site	**code**	**latitude**	**longitude**	**time period**
Rincón del Bonete	RB	-32.800	-56.416	04/2010 :: 04/2011
Buena Unión	BU	-31.058	-55.602	04/2010 :: 04/2011
Piedras de Afilar	PA	-34.682	-55.575	01/2010 :: 04/2011

Hourly data were carefully inspected for consistency and a small number of hours were discarded. Hourly data with zenith angle outside the allowed range or with clearness index greater than 0.8 was filtered out. The training and the evaluation processes both require simultaneous hourly irradiation records and valid satellite images for that hour and location. We discarded irradiation data corresponding

to hours and locations were satellite images were not available. Daily totals were only generated for days with complete hourly records, *i.e.* no interpolation scheme for missing hours was used. Monthly averages were generated only for months with more than 15 valid daily records. After this filtering stage, our training dataset is composed of 9831 hourly records, 555 daily records and 19 monthly records and the evaluation set comprises 11317 hourly records, 578 daily records and 21 monthly records.

3. Tarpley's model

The estimation of solar irradiation from satellite imagery has a rather long history. In the early times, two kinds of models were distinguished: statistical and physical models. In the first case, a small number of parameters are adjusted using ground data. In the second case, the radiative transfer process of solar radiation in the atmosphere is described in a simplified form and input of some atmospheric or meteorological data is usually required, such as precipitable water or ozone concentration. Physical models also require conversion of the brightness counts from the satellite image into flux density of upward solar radiation emerging from the atmosphere and this requires a careful calibration of the satellite radiometer. Both approaches have their strengths and weaknesses, see M. Noia et al. (1993a,b) for a useful review and discussion on the early models. Modern implementations are often of a hybrid nature and use a physical model in which a few parameters are adjusted using ground measurements.

Tarpley's model is a statistical model which, due to its simplicity, is suitable for a first step in using satellite imagery to estimate solar irradiation. In fact, we shall conclude that it has an attractive balance between simplicity and accuracy. It was first introduced by Tarpley as part of the Great Plains experiment Tarpley (1979). It was observed that a bias effect in the model produced overestimates at low insolation values and underestimates at high insolation, so a revised algorithm was proposed by Tarpley and co-workers Justus et al. (1986). In an hourly basis,

$$I = I_{sc}\,(r_0/r)^2 \cos\theta_z \left(a + b\cos\theta_z + c\cos^2\theta_z\right) + d\left(B_m^2 - B_0^2\right), \tag{1}$$

where I is the hourly global solar irradiation on a horizontal plane at ground level (in $\mathrm{MJ/m^2}$) and $I_{sc} = 4.921\,\mathrm{MJ/m^2}$ is the hourly integral of the Solar Constant. The factor $(r_0/r)^2$, accounts for the variation of the Sun-Earth distance (assumed constant within a day) and depends on the Julian day number Duffie and Beckman (2006). The solar zenith angle, θ_z, is the angle formed by the Sun–observer direction with the local vertical. It depends on the position (latitude, longitude) and on the day and standard time of the observer. The hourly averages of $\cos\theta_z$ and its powers, to be used in Eq. (1), were evaluated from their exact expressions, although for the accuracy of the model the hourly mid-point values could have been used equally well. The terms with the coefficients a, b and c represent the clear-day part of the model and the last term in Eq. (1) provides the cloud cover information from satellite images. B_m is proportional to the mean observed brightness at a given time and location and B_0 is the corresponding brightness (for the same time and location) in the absence of clouds, i.e. the clear day brightness. The presence of clouds enhances reflexion and results in $B_m > B_0$ so d is expected to be negative.

Tarpley and collaborators used a set of 7200 coincident satellite and pyranometer hourly observations over the USA Great Plains area to determine the four coefficients in Eq. (1) by linear regression.

$$a = 0.4147, \quad b = 0.7165, \quad c = -0.3909, \quad d = -1.630\ \mathrm{kJ/m^2}. \tag{2}$$

They used GOES-East satellite images and this set of coefficients to generate irradiation estimates for 17 months (in 1982-1983) for the Central Plains of the United States, Mexico and part of South America with $1^\circ \times 1^\circ$ resolution in a spatial region that includes the whole Uruguayan territory.

The rms errors observed against their own training sites but for different time periods are low. On a daily basis, for 1021 site-days with a mean of $14.6\,\mathrm{MJ/m^2}$ they report an absolute rms error of $1.6\,\mathrm{MJ/m^2}$ or 10.9% of the mean Justus et al. (1986).

3.1 Model performance

The performance of a statistical model should ideally be obtained from a comparison against data sets which are not part of the training set used to derive the coefficients. Tarpley and collaborators Justus et al. (1986) (JTP) evaluated the performance of Eq. (1) on an hourly basis, with 7200 observations for the period August–December 1980, and report an rms error of 16.2% of the observed mean. On a daily basis, against a set of 282 ground-based pyranometer measurements from a single site at Atlanta, Georgia (33.8 °N, 84.4 °W), they report a rms relative to the observed mean of 12.6 %. JTP quote other independent comparisons with ground daily irradiation data for the U.S. for some days in 1983 which yielded worst results. Some of the discrepancies have been traced to the difficulty in distinguishing brightness from clouds from brightness resulting from snow cover when using images from the visible channel only. Finally, JTP also quote results of a comparison made at four sites in Argentina by Espoz and Brizuela, who reported a 13.6% rms relative to the observed daily mean. These early results are summarized in Table 4.

Frulla and collaborators compared daily estimates from Tarpley's model, using the coefficients from Eq. (2), to measurements from several stations in Argentina Frulla et al. (1988) and the southern part of Brazil Frulla et al. (1990) and they reported rather high rms deviations. In Argentina, 5322 daily measurements from 13 stations for 1982-1983 were compared with daily estimates from Tarpley's model at each location. The absolute rms was 3.2 $\mathrm{MJ/m^2}$ and the observed mean 16.3 $\mathrm{MJ/m^2}$ implying an rms of 19.6% relative to the mean Frulla et al. (1988). In Brazil, a similar study compared 4404 site-days from 9 stations for 1982-1983 with Tarpley's model estimates for each site. An rms error of 3.2 $\mathrm{MJ/m^2}$ was reported, for an observed mean of 15.8 $\mathrm{MJ/m^2}$. This corresponds to a relative rms error of 20.3%. These studies also show that the errors obtained from clear days are lower than for cloudy days. These results, also summarized in Table 4, show that the rms errors are lower when the coefficients are locally estimated, i.e. in the U.S. Central Plains area. This suggests that the coefficients in Eq. (1) should not be regarded as universal, even for regions with similar climate and geographical characteristics.

An implementation in which Tarpley's coefficients were calculated locally Righini and Barrera (2008) was done using images from the GOES-8 satellite and data from 5 pyranometric stations in Argentina. The images covered nine months within the 2000-2002 period. They use the methodology described in detail in Justus et al. (1986) to determine a modified clear day brightness, B_0. Noting that the model tends to estimate better solar irradiation for clear days, the authors chose to treat separately clear days, partially cloudy days and cloudy days, discriminating them solely on the basis of the value of the daily clearness index. The daily irradiation estimates obtained from the satellite images and ground data for a total of 715 site-days were compared with the data in the training set. With this methodology, they report a relative rms error of 17.3% on a daily basis (8.9% on a monthly basis). Inspection of Table 4 shows that these preliminary results represent an improvement over previous estimates for the south american region Frulla et al. (1988, 1990); Righini and Barrera (2008).

3.2 Local implementation

The previous discussion suggests that Eq. (1) performs significantly better when the set of coefficients $(a, b, c, d$ and the clear day brightness field, $B_0)$ are locally determined. In order to keep the model simple and as general as possible, we do not treat clear day data separately. Thus, we shall use ground data to obtain a single set of coefficients for Eq. (1), and they are assumed to be time-independent and valid for the whole territory under consideration.

Effects such as cloud dynamics and small changes in satellite orientation are reduced by averaging the brightness counts over a spatial neighborhood for every location of interest. We use neighborhoods of $10' \times 10'$ cells which correspond to a ground area of about 16 km $\times$19 km. We use use the same cell sizes for adjusting the model and to generate irradiation estimates, so this is the spatial resolution of these estimates. For each cell, centered at the latitude and longitude (ϕ, ψ) of a given location, the mean brightness B_m is calculated as the simple average of all pixels in the cell using all the available images

Table 4: Performance of Tarpley's model for several locations.

basis	**data points**	**time period**	**observed mean** (MJ/m^2)	**absolute rms error** (MJ/m^2)	**relative rms error** (%)	**Sites**	**Reference**
hourly	7200	08-12/1980			16.2		Justus et al. (1986)
daily	1021	08-12/1980	14.6	1.6	11.0		Justus et al. (1986)
daily	282	1982	15.1	1.9	12.6	1	Justus et al. (1986)
daily	765	1982	15.7	2.1	13.6	5	Espoz and Brizuela (1983)
daily	195	01-05/1983		2.8		2	Riordan (1984)
daily	1240	03-09/1983		3.0		7	Sullivan et al. (1984)
daily	5322	1982-1983	16.3	3.2	19.6	13	Frulla et al. (1988)
daily	4404	1982-1983	15.8	3.2	20.3	9	Frulla et al. (1990)
daily†	715	2000-2002			17.3	5	Righini and Barrera (2008)
monthly	18	1982-1983	14.8	0.8	5.4	1	Justus et al. (1986)
monthly†	30	2000-2002			8.9	5	Righini and Barrera (2008)

(†) comparison made against the same data used to adjust the model's parameters.

within the hour. In this way, a B_m field is obtained for each hour (local time), for each date and location. For instance, all images and ground data for the time interval 10:30 to 11:29 are assigned to the hour 10.

In order to determine the clear day brightness B_0 for each cell, we follow the procedure outlined in Tarpley (1979). The time dependence of the B_0 field for a cell at (ϕ, ψ) is parametrized as

$$B_0(\phi,\psi) = A(\phi,\psi) + B(\phi,\psi)\cos\theta_z + C(\phi,\psi)\sin\theta_z\cos\gamma + D(\phi,\psi)\sin\theta_z\cos^2\gamma \tag{3}$$

where γ is the azimuth angle between the Sun and satellite directions for the chosen observation point (ϕ, ψ). According to Tarpley (1979), the second term in Eq. (3) accounts for the changing incident flux with local time, day and location. The other two terms are an attempt to account for changes in target brightness due to surface shadows and anisotropic scattering. Ideally, the coefficients in Eq. (3) should be adjusted using images for clear days only.

The B_m data which corresponds to hours contaminated with clouds or to insufficient scene illumination were filtered out using the following iterative procedure:

1. Cells with corrupted B_m values or with $\cos\theta_z < 0.1$ (corresponding to high air masses and possibly long shadows) are filtered out.

2. As an initial guess for the B_0 field we choose $B^* = 2500$ counts, with no time or cell dependence. This value was chosen after visual inspection of several histograms of B_m values for different locations.

3. The tails of the distribution of B_m are filtered out: cells with B_m values such that $|B_m - B^*| > \sigma/2$ are excluded, where σ is the standard deviation of the current B_m set.

4. From the reduced set of B_m, a first set of coefficients (A_0, B_0, C_0, D_0) is obtained for each cell, by linear regression from Eq. (3) and the residuals $\epsilon_0 = |B_m - B_0|$ are computed. High residuals are probably either from cloud contaminated or from poorly illuminated cells, so cells for which $\epsilon_0 > c_0\sigma_0$ are discarded.

5. An updated field of coefficients (A_k, B_k, C_k, D_k) is obtained by regression, using the remaining set of B_m, from the previous stage. The residuals are updated and cells with $\epsilon_k > c_k\sigma_k$ are discarded.

6. The previous step is iterated, for $k = 1, 2, 3\ldots$, until the fractional variation in the coefficients is below a certain threshold.

The choice $c_0 = 1.2$ and $c_k = c_0 + 0.1 \times k$ causes the above procedure to terminate after a few iterations. Notice that the bound on the absolute residuals ϵ_k is being reduced. The whole process is repeated for each location of interest and, finally, a field of coefficients (A, B, C, D) is obtained. Then, one can use Eq. (3) to obtain B_0 values at the required location, date and time.

Table 5: Coefficients for Eq. (1), obtained from the training set (Table 2).

	a	b	c	d (kJ/m^2)
this work	0.3016	0.8628	-0.4101	-0.760
Justus et al. (1986)	0.4147	0.7165	-0.3909	-1.630

An actualization of the B_0 field value was introduced in Justus et al. (1986). It involves the application of a function $B_0' = F(B_0, B_m)$, defined in terms of thresholds $B_{max}, B_{min}, B_\delta$ and weights w_1 and w_2 to an initial guess for B_0. We have implemented this procedure with $B_{max} = 3200$ counts, $B_{min} = 1400$ counts and $B_\delta = 300$ counts, $w_1 = 0.99$ and $w_2 = 0.90$. The application of this actualization rule did not lead to a significant improvement in our model's performance, so we do not use this procedure for the results reported in this work.

Using hourly values of $\cos\theta_z$, B_m and B_0, together with ground measurements of hourly global irradiation from the training set (Table 2), the model described by Eq. (1) was fitted using a standard least–squares technique. In order to avoid that the coefficients (a, b, c, d) have very different magnitudes, we normalized brightness counts with a factor of 2^8. The 9831 hourly data records from the training sites (Table 2) were filtered for $\cos\theta_z > 0.1$ to eliminate hours with insufficient illumination. The remaining set of 9149 hours was used to adjust the model coefficients listed in Table 5. Except for d, that depends on the scaling used for the brightness values and on the units used for the solar irradiation data, these values are similar to those obtained by Tarpley and co-workers for the Great Plains Justus et al. (1986). The general geographical characteristics of our target territory (smooth grasslands with no snow cover, deserts or significant heights) are similar to those of the U.S. Great Plains, so similar values for the coefficients associated to the clear–sky part of the model were to be expected.

With these coefficients and the B_0 field determined from Eq. (3) for a given location, one can use the mean brightness, B_m, from satellite images in Eq. (1) and generate hourly estimates of irradiation for that location.

4. Solar irradiation assessment

Hourly irradiation estimates were generated from Eq. (1) for the six locations in which we have ground data. In Fig. 2 we compare the hourly irradiation estimates with the corresponding measurements for one of the sites in our testing set (Rincón del Bonete–RB). Agreement is best for clear days as expected from the structure of Eq. (1) which is essentially a clear-day model supplemented with a term that substracts irradiation due to the presence of clouds.

The model performance is evaluated by calculating the average root mean square deviation, E_{rms}, which for N pairs of model estimates and measured values $(\hat{X}_i, X_i)$ is defined in the usual way,

$$E_{rms} \equiv \sqrt{\frac{1}{N}\sum_{i=1}^{N}\left(X_i - \hat{X}_i\right)^2}. \tag{4}$$

This quantity, evaluated on an hourly, daily or monthly basis, will be used as a figure of merit to asses the model performance. We also report the relative (rms) error, $\epsilon_{rms} = E_{rms}/\bar{X}$, expressed as a percentage of the mean value, $\bar{X}$, of the measured irradiation on the corresponding basis. The model is expected to perform significantly better against the training data set than against data from the testing stations. We have included the comparison with the testing set in order to compare with other recent implementations of Tarpley's model which use this measure of performance. For instance, in Righini and Barrera (2008) a

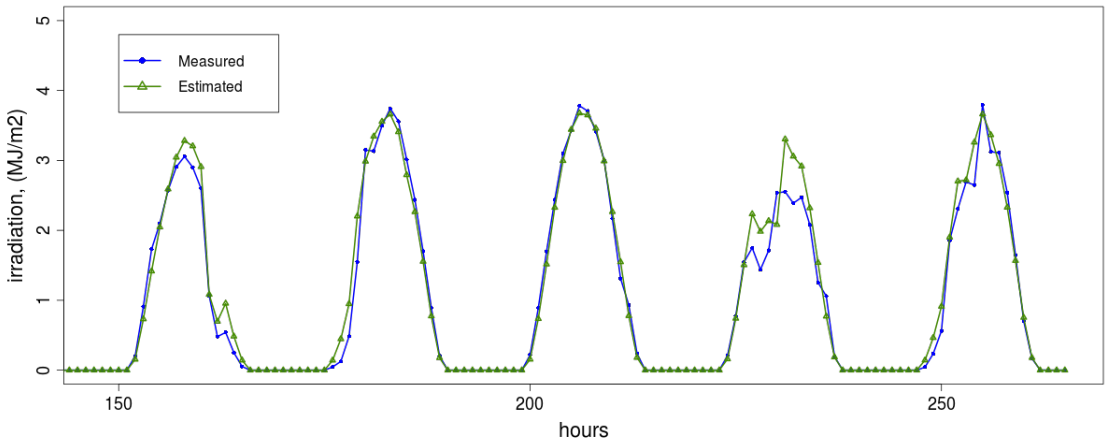

Figure 2: Measured irradiation and irradiation estimated from Eq. (1) for five consecutive days of November 2010. The comparison is on an hourly basis and the data is from the RB site.

local implementation of Tarpley's model with rms deviations of 17.3% (daily) and 8.9% (monthly) with respect to the training set has been reported.

4.1 Hourly Comparison

In Table 6, we show a comparison of hourly irradiation estimates and measurements for 11317 site-hours from our testing set. A rms deviation of 0.29 MJ/m^2 or 19.8% of the observed mean of 1.45 MJ/m^2 was obtained. The relative rms reduces to 16.2% when compared with data from the training set. Fig. 3 shows the scatter plots for hourly irradiation for hours in each set. Inspection of this scatter plots show that the model tends to over-estimate solar irradiation for cloudy days and under-estimate irradiation for clear days.

Table 6: Comparison between the model estimates for hourly irradiation and recorded ground data. Sites in the training (1) and testing (2) sets are considered separately and the mean $\bar{I}$ is for the measured data. See Tables 2 and 3 or Fig. 1 for station locations.

Site	**Code**	**Type**	N (hours)	$\bar{I}$ (MJ/m^2)	E_{rms} (MJ/m^2)	ϵ_{rms} (%)
Las Brujas	LB	1	3218	1.50	0.24	16.2
Treinta y Tres	TT	1	3390	1.54	0.25	16.0
Salto	SA	1	3323	1.55	0.25	16.4
All (training set)			**9931**	**1.53**	**0.25**	**16.2**
Rincón del Bonete	RB	2	3835	1.53	0.24	15.7
Buena Unión	BU	2	3889	1.41	0.30	21.1
Piedras de Afilar	PA	2	3593	1.39	0.32	22.8
All (testing set)			**11317**	**1.45**	**0.29**	**19.8**

For a few hours in the training set, the model generated non-physical negative irradiation values. We tried to avoid this issue by implementing a constrained regression technique Coleman and Li (1996); Gill et al. (1981), so that the resulting irradiation estimates at the training sites would necessarily be positive. This modification produced a reduced overall accuracy and negative irradiation estimates could still be obtained at sites which are not in the training set. Thus, for the sake of simplicity, we used the standard least–squares technique and set $I = 0$ whenever the original estimate is negative, as required

for consistency with physical constrains for the problem.

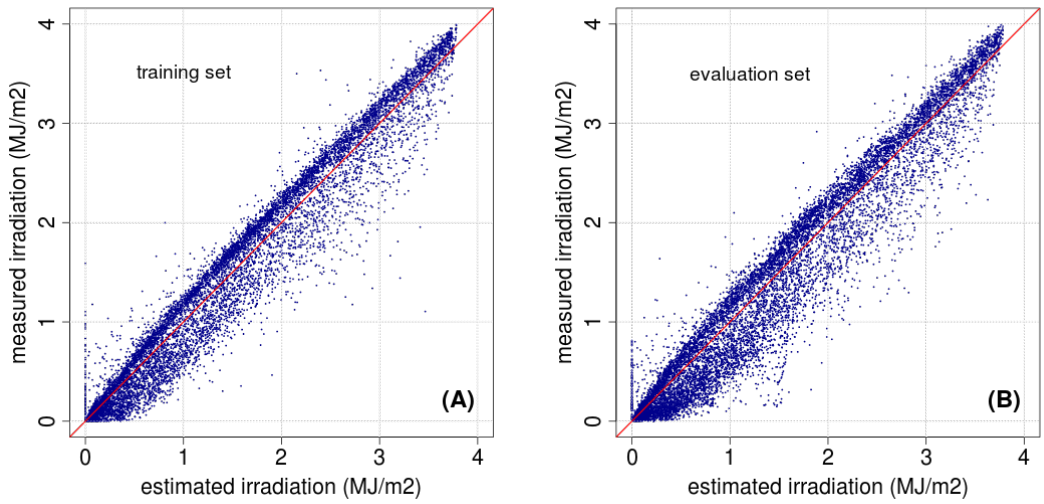

Figure 3: Scatter plots for hourly ground data vs. hourly estimates from Eq. (1) for: (A) all valid hours in the training set and (B) all valid hours in the evaluation set. A diagonal line has been drawn to guide the eye.

4.2 Daily Comparison

The comparison on a daily basis is summarized in Table 7. It was done for 578 days in our testing set (days in which one or more hours of data where missing were discarded). A rms deviation of 2.2 MJ/m^2 or 11.8% of the observed daily mean of 18.4 MJ/m^2 was obtained. The relative rms reduces to 9.3% when compared with data from the training set. Deviations for the RB station data are remarkably low and comparable to those from the training set. One possible explanation for this good performance may be that the RB site is located in the midpoint of the area defined by the three sites of the training set, see Fig. 1. The corresponding scatter plots for comparison on a daily basis are shown in Fig. 4. The over-estimation of solar irradiation for cloudy days and the under-estimation for clear-days can be seen more clearly in the daily scatter plot.

Table 7: Comparison between the model estimates for total daily irradiation and the recorded ground data. Sites in the training (1) and testing (2) sets are considered separately and the mean $\bar{H}$ is for the measured data. See Tables 2 and 3 or Fig. 1 for station locations.

Site	**Code**	**Type**	N (days)	$\bar{H}$ (MJ/m^2)	E_{rms} (MJ/m^2)	ϵ_{rms} (%)
Las Brujas	LB	1	175	18.50	1.83	9.9
Treinta y Tres	TT	1	194	19.54	1.68	8.6
Salto	SA	1	186	19.74	1.90	9.6
All (training)			**555**	**19.28**	**1.79**	**9.3**
Rincón del Bonete	RB	2	202	19.40	1.77	9.1
Buena Unión	BU	2	224	18.24	2.26	12.4
Piedras de Afilar	PA	2	152	17.08	2.49	14.6
All (testing)			**578**	**18.36**	**2.17**	**11.8**

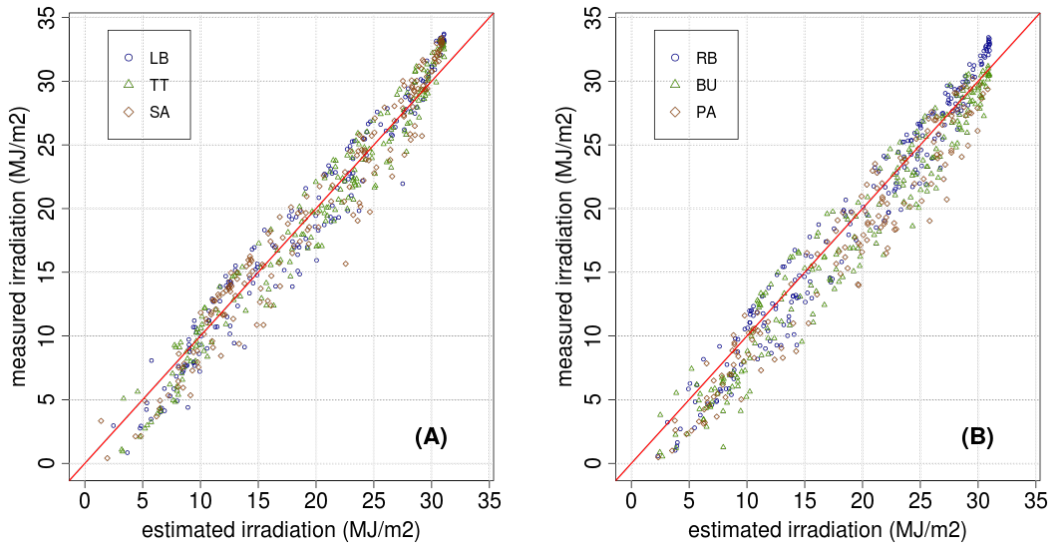

Figure 4: Scatter plots for daily ground data vs. daily estimates from Eq. (1) for: (A) all valid days in the training set and (B) all valid days in the evaluation set. A diagonal line has been drawn to guide the eye.

Table 8: Comparison between the model estimates for mean monthly irradiation and the recorded ground data. Sites in the training (1) and testing (2) sets are considered separately and the mean $\bar{H}$ is for the measured data. See Tables 2 and 3 or Fig. 1 for station locations.

Site	**Code**	**Type**	N (months)	$\bar{H}$ (MJ/m^2)	E_{rms} (MJ/m^2)	ϵ_{rms} (%)
Las Brujas	LB	1	6	18.75	0.73	3.9
Treinta y Tres	TT	1	7	21.42	0.54	2.5
Salto	SA	1	6	20.56	1.05	5.1
All (training)			**19**	**20.31**	**0.79**	**3.9**
Rincón del Bonete	RB	2	7	20.32	0.79	3.9
Buena Unión	BU	2	8	19.05	1.45	7.6
Piedras de Afilar	PA	2	6	21.03	1.83	8.7
All (testing)			**21**	**20.04**	**1.40**	**7.0**

4.3 Monthly Comparison

The results of the comparison for monthly averages are summarized in Table 8. Due a problem which affected the measuring stations, there were several days missing in many months. Thus, we adopted the rather loose criteria of calculating a monthly average if there were at least 15 valid days of data for that month. For 21 site-months in our testing set, the monthly rms deviation was 1.4 MJ/m^2 or 7% of the observed mean of 20 MJ/m^2. The corresponding scatter plot is shown in Fig. 5. The comparison of monthly average daily irradiation for months from the training set and from the testing set is shown in the same plot. The site for each point is identified in the legend.

This is a report on work in progress and we have not yet done a detailed analysis of our results. However, the rms daily deviations of 11.8% are comparable to the ones obtained by Tarpley (12.6%, see Table 4) with respect to the independent Georgia data Justus et al. (1986). Inspection of Table 4 shows that the rms deviations obtained from this preliminary work are comparable to the best implementations of Tarpley's model so far.

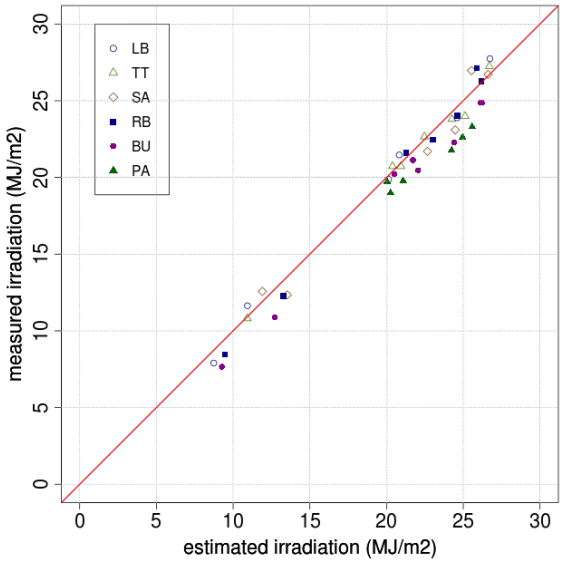

Figure 5: Scatter plot for monthly averages from ground data vs. monthly estimates based on Eq. (1). Both the training set and evaluation set data points are shown. A diagonal line has been drawn to guide the eye.

5. Conclusions

A set of GOES-13 (2010-2011) images and simultaneous irradiation data from six stations in our target territory were used to determine the four parameters in Tarpley's model. The clear-day brightness field B_0 was determined from the set of images using an iterative filtering procedure designed to filter out images with traces of clouds or with insufficient illumination. Hourly estimates of irradiation were generated for the six sites where we have simultaneous recorded ground data. Estimated irradiation values were compared on an hourly, daily and monthly basis with ground measurements. Data from three sites equipped with new CMP6 field pyranometers was used as the training set and data from three other sites, equipped with new Li-Cor sensors, was used as the testing set. The rms deviations between the estimate and the observation were calculated for each of these data sets. The relative rms deviates obtained from comparison with the testing set data are approximately 20%, 12% and 7% of the mean on an hourly, daily and monthly basis respectively.

We find these results encouraging, but this is a report on work in progress and there is further room for improvement and refinement. First, the proper calibration of GOES images should allow us to increase the number of valid data records and the scope of the model. For instance, long term (10-year) estimates of solar irradiation could be obtained and compared with existing long term measurements. Second, the crucial process for determining the clear-day brightness field can be further refined using standard filtering procedures based on robust estimation from the image processing area, such as RANSAC, Fischler and Bolles (1981). Third, since the model performs better for clear days, a cloud-index dependence can be taken into account when determining the set of coefficients, so that using data in each category, three sets (clear day, partly cloudy and cloudy) of coefficients can be obtained. A similar approach, based on the clearness index, was followed in Righini and Barrera (2008).

This work shows that Tarpley's model has a good balance between simplicity and performance. As with other statistical irradiation models, the quality of its output relies on the quality of the data that is used to adjust and test it. We hope to refine these preliminary results as more controlled quality ground-based measurements become available.

Aknowledgements: We thank Daniel Larrosa, Eliana Cornalino and Martín Draper Vanrell (UTE) for kindly providing us with the ground data, partoof which was used as the testing set for this work.

*

References

Abal, G., D'Angelo, M., Cataldo, J., and Gutierrez, A. (2010). Mapa Solar del Uruguay. In *Anals of the IV^{th} Latin-American Conference on Solar Energy (IV ISES-CLA)*, Cusco, Perú.

Angström, A. (1924). Solar and terrestrial radiation. Report to the international commission for solar research on actinometric investigations of solar and atmospheric radiation. *Q. J. Royal Meteorological Society*, 50(210):121 – 126.

Coleman, T. and Li, Y. (1996). A reflective newton method for minimizing a quadratic function subject to bounds on some of the variables. *SIAM Journal on Optimization*, 6(4):1040–1058.

D'Angelo, M., Toscano, P., Abal, G., and Ceballos, J. (2011). Spatial distribution of daily mean global solar irradiation in uruguay. In *Annals of the Solar World Congress (SWC 2011)*, Kassel, Germany.

Duffie, J. and Beckman, W. (2006). *Solar Engineering of Thermal Processes*. Wiley and Sons, Hoboken, New Jersey, third edition.

Espoz, C. and Brizuela, A. (1983). Application of remote sensing and agrometeorological methods for crop assesment in the pampa húmeda. Technical Report ARG 81/002, FAO.

Fischler, M. and Bolles, R. (1981). Random sample consensus: a paradigm for model fitting with applications to image analysis and automated cartography. *Communications of the ACM*, 24(6).

Frulla, L., Gagliardini, A., Grossi Gallegos, H., and Lopardo, R. (1988). Incident solar radiation on argentina from teh gesotationary satellite GOES: comparison with ground measurements. *Solar Energy*, 41(1):61–69.

Frulla, L., Grossi Gallegos, H., Gagliardini, D., and Atienza, G. (1990). Analysis of satellite-measured insolation in Brazil. *Solar & wind technology*, 7(5):501–509.

Gill, P. E., Murray, W., and Wright, M. (1981). *Practical Optimization*. Academic Press, London, UK.

Justus, C., Paris, M., and Tarpley, J. (1986). Satellite-measured insolation in the United States, Mexico, and South America. *Remote Sensing of Environment*, 20(1):57–83.

M. Noia, M., Ratto, C., and Festa, R. (1993a). Solar irradiance estimation from geostationary satellite data: 1. statistical models. *Solar Energy*, 51:449–456.

M. Noia, M., Ratto, C., and Festa, R. (1993b). Solar irradiance estimation from geostationary satellite data: 2. physical models. *Solar Energy*, 51:457–465.

Prescott, J. (1940). Evaporation from a water surface in relation to solar radiation. *Trans. R. Soc. Sci. S. Austr*, 64:114–118.

Righini, R. and Barrera, D. (2008). Empleo del modelo de tarpley para la estimación de la radiación solar global mediante imágenes satelitales goes en argentina. *Avances en Energías Renovables y Medio Ambiente*, 12:9–15.

Riordan, C. (1984). A preliminary comparison of insolation measurements, forecasts and estimates from satellite imagery. Technical Report TR-215-2046, SERI.

Sullivan, G., French, V., LeDuc, S.K. Sevaug, J., and Wilson, W. (1984). Evaluation of satellite-derived estimates of solar radiation. Technical Report JSC-20240, AgRISTARS.

Tarpley, J. (1979). Estimating incident solar radiation at the surface from geostationary satellite data. *Journal of Applied Meteorology*, 18:1172.

Toscano, P. and Cataldo, J. (2011). Solar irradiation measurement in uruguay. In *Annals of the Solar World Congress (SWC 2011)*, Kassel, Germany.